ChemComm

Accepted Manuscript

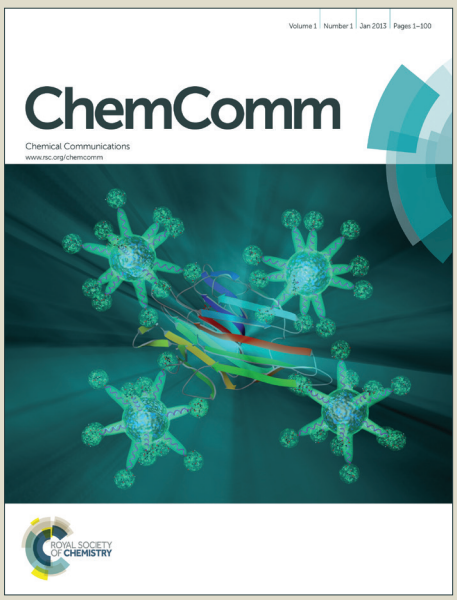

ROYAL SOCIETY OF CHEMISTRY

www.rsc.org/chemcomm

ChemComm

RSCPublishing

COMMUNICATION

Solution-grown single-crystalline microwires of a molecular semiconductor with improved charge transport properties

Cite this: DOI: 10.1039/x0xx00000x

Received 00th January 2012,
Accepted 00th January 2012

DOI: 10.1039/x0xx00000x

www.rsc.org/

Akshaya K. Palai,†[a] Jihee Lee,†[a] Tae Joo Shin,[b] Amit Kumar, [a] Seung-Un Park,[a] Seungmoon Pyo*[a]

Preparation and structural analysis of highly ordered single crystalline wires of diketopyrrolopyrrole (DPP) molecular semiconductor grown through a solution process is reported, and the static/dynamic electrical response of organic electronic device using the DPP semiconductor has been analyzed.

Conjugated organic materials that can be self-assembled into nano/micro structures[1] and easily processed from solution are useful for high performance organic field-effect transistors (OFETs).[2] Among the various conjugated organic materials, diketopyrrolopyrroles (DPPs) were recently considered as suitable materials for OFETs[3] owing to their flexible processability and attractive optoelectronic properties. Recently, OFETs based on molecular DPPs containing alkylated thiophenes prepared by solution processes over *n*-octadecyltrichlorosilane (OTS)-modified Si/SiO_2 have been reported with a field-effect hole mobility of ~10^{-2} to ~10^{-3} $cm^2/V \cdot s$.[4,5] However, the use of 1D-micro/nanostructures obtained from DPP derivatives for fabricating solution-processable efficient OFETs is limited.[6] In addition, OFETs and complementary inverters that are based on the micro/nano-structures of molecular DPP on solution-processable gate dielectric, are very rare. In this communication, we present a simple solution-based approach for the preparation of single-crystalline microwires of 2,5- dihexadecyl-3,6-bis(5-(3-hexylthiophen-2-yl)thiophen-2-yl)pyrrolo[3,4-c]pyrrole-1,4(2H,5H)-dione (**DPP(3HT)$_2$** (chemical structure is shown in Fig. 1). The charge transport behaviors of OFETs and complementary inverters with a solution-processable gate dielectric were investigated by measuring their static and dynamic electrical response, in addition to analyzing the structure of single crystalline **DPP(3HT)$_2$** microwires using grazing-incidence X-ray diffraction (2D-GIXD) and this structure with that of **DPP(3HT)$_2$** thin film. Our single crystalline microwires based organic transistor and inverter exhibit a high mobility of 0.40 $cm^2/V \cdot s$ with an on/off ratio of 10^3 and a high gain of 18, respectively.

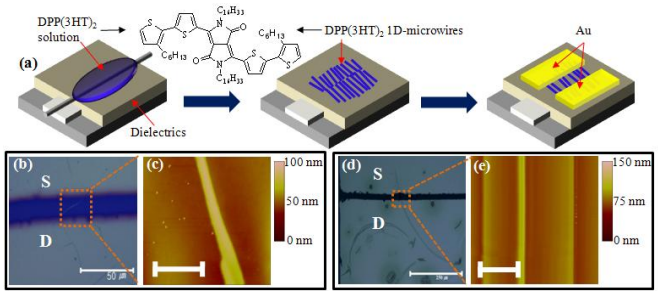

Fig. 1 A schematic fabrication procedure for **DPP(3HT)$_2$** microwire- based OFET (a). The OM images (b and d) (scale bar 50 μm) and AFM images (c and e) of a DPP(3HT)$_2$ single microwire grown on Si/SiO_2 (5×5 μm^2, scale bar 2 μm) and CL-PVP/ITO (15×15 μm^2, scale bar 5 μm) substrate.

Fig. 1a shows a schematic representation of OFETs based on the **DPP(3HT)$_2$** single-crystalline microwires prepared by the solution dewetting method.[7] Two types of gate dielectrics, SiO_2 (100 pF/mm^2) and cross-linked poly(4-vinly phenol) (CL-PVP) (61.04 pF/mm^2), were employed. The channel width (W) was calculated by measuring the contact area of the **DPP(3HT)$_2$** wires lying between the source and drain electrodes. The channel length (L) was fixed to 20 μm. The position and shape of **DPP(3HT)$_2$** wires were investigated by atomic force microscopy (AFM) and optical microscopy (OM) images from which are shown in Figs. 1b-e and Figs. S1(a-e, ESI‡). The images confirm that the **DPP(3HT)$_2$** wires lie between the electrodes of the OFETs. The OM and AFM images of one (Fig 1b-c) and two (Fig S1a-c, ESI‡) **DPP(3HT)$_2$** wire based OFETs on Si/SiO_2 substrate are shown. The output (I_{DS} - V_{DS}) and transfer (I_{DS} - V_{GS}) curves of the OFETs with multiple wires show typical *p*-type charge transport behavior as depicted in Figs. S2a and b (ESI‡). The best and average field-effect hole mobility (μ_h) of the device was 0.40 and 0.12 $cm^2/V \cdot s$, almost 200 and 60 times higher than that of **DPP(3HT)$_2$** film based devices[8], respectively and even higher compared to the reported values of DPP crystal based OFETs.[9] Average values of μ_h, V_{th}, I_{on}/I_{off}, and ss as calculated from 13 devices are ~0.12 $cm^2/V \cdot s$, 7.00 V, 2.03 × 10^3 and 10.60 V/dec, respectively. We also successfully fabricated OFETs with a single **DPP(3HT)$_2$** wire, the output and transfer characteristic curves of

which are shown in Figs S2c and d (ESI‡), respectively. The maximum values achieved of μ_h, V_{th}, I_{on}/I_{off}, and ss were ~0.15 $cm^2/V \cdot s$, 7.70 V, 9.93 × 10^1 and 5.50 V/dec, respectively. Detailed device performance parameters are summarized in Table S1 (ESI‡).

In order to investigate the electrical behavior of the DPP wire on polymer gate dielectric, essential for flexible organic devices, **DPP(3HT)$_2$** single-crystalline wires were also grown on the CL-PVP gate dielectric, and the device's performance was analyzed. The OM and AFM images of the single (Fig 1d-e) and four (Fig S1d-e, ESI‡) **DPP(3HT)$_2$** wire-based OFETs with CL-PVP are shown. The characteristic curves of devices with multiple wires are shown in Fig. S3a and b (ESI‡), respectively. Such OFETs showed typical *p*-channel behavior and a moderate saturation behavior. The maximum values achieved of μ_h, V_{th}, I_{on}/I_{off}, and ss of the OFET were estimated to be ~0.14 $cm^2/V \cdot s$, 4.3 V, 2.03 × 10^2, and 8.5 V/dec, respectively. Compared to **DPP(3HT)$_2$** thin-film based OFETs, the mobility of such OFETs increased by ~75 (from best mobility) and 25 (from average mobility, table 1) times, which is comparable or higher to those previously reported other functionalized DPP derivatives.[10]

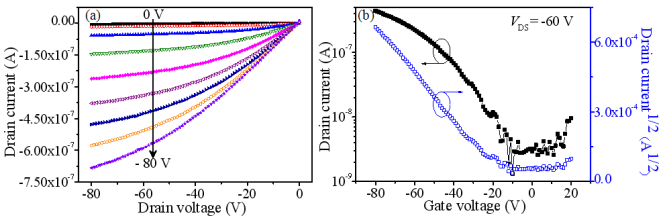

Fig. 2 Output (a) and transfer (b) characteristics of the OFET (L/W = 20/10.7 μm) with a single 1D-microwire of **DPP(3HT)$_2$** on CL-PVP gate dielectric.

In addition, air stability of the devices was investigated as shown in Fig. S4 (ESI‡) by measuring device's (having 4 wires) performance after storage for 65 days in air. Upon such air storage, mobility decreased moderately to 0.01 $cm^2/V \cdot s$, but still showed good *p*-channel properties. We also successfully fabricated a device with a single **DPP(3HT)$_2$** wire grown on CL-PVP. The device's characteristic curves are shown in Figs. 2a and b. The maximum achieved values of μ_h, V_{th}, I_{on}/I_{off}, and ss are ~0.08 $cm^2/V \cdot s$, -15.2 V, 1.52 × 10^2, and 20.5 V/dec, respectively. We found that the performance of devices based on crystalline wires were much better than that of film-based devices. In order to correlate the structures of **DPP(3HT)$_2$** in its thin-film and crystalline wire forms with device performance, two-dimensional grazing incidence X-ray diffraction (2D-GIXD) experiments were performed (detailed in ESI‡). Fig. 3a and b show the GIXD images of DPP(3HT)$_2$ wire and 50-nm thick film on CL-PVP/ITO substrate, respectively. In Fig. 3a, characteristic spot-like strong diffractions are clearly seen, strongly suggesting the single crystalline nature of wire. On the other hand, the GIXD patterns of the thin-film exhibit very broad and diffused peaks as in Fig. 3b, indicative of either amorphous-like features or a crystalline nature with low crystallinity. Fig. 3b shows extra diffraction peaks at an angle of ~69° from the surface normal. (the dotted ellipsoids in Fig. 3b). Out-of-plane 1D-GIXD profiles at q_{xy} = 0 (q_z-profiles) are plotted in Fig. 3c.

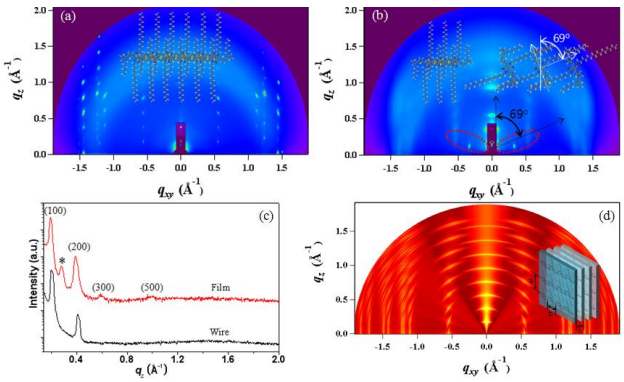

Fig. 3 2D-GIXD images of **DPP(3HT)$_2$** (a) microwire and (b) 50 nm-thick film on CL-PVP/ITO substrate. The q_z-profiles extracted from (c) measured GIXD data and (d) simulated 2D-GIXD images.

The q_z-profile of a wire shows two distinct peaks at q_z = 0.2111 and 0.4215 Å^{-1}, which can be assigned as the 1st and 2nd order diffraction peaks associated with a lamellar structure with 29.8 Å layer spacing. Thin-film shows diffraction peaks at q_z = 0.1961, 0.3932, 0.5894, 0.9890, and 0.2811 Å^{-1} (indicated by * in Fig. 3c). These peaks (assigned as [*h00*] diffractions) are attributable to the 1st and higher order peaks of a lamellar structure with 32.0 Å interlayer spacing. In order to understand these diffraction patterns, the molecular structure of **DPP(3HT)$_2$** was considered. A **DPP(3HT)$_2$** molecule consists of rigid central DPP conjugation unit about 18 Å -long, and long alkyl side of length 7.6 Å (C6) and 20.3 Å (C16) attached perpendicularly to the conjugation unit. The fully extended molecular length along the long side alkyl chains is calculated to be about 45 Å . So, when a **DPP(3HT)$_2$** molecule is regularly aligned on the surface, in which long side alkyl chains are normal to the surface and the edge of conjugation unit is parallel to the surface (see, a schematic model in Fig. 3a, inset, enlarged one in Fig. S5. ESI‡), its single layer spacing is 45 Å . However, if the molecule is slighted tilted (less than 5°) on the surface and side long alkyl chains are interdigitated between the lower and upper layer by about 13 ~ 15 Å (3/4th the size of the long side alkyl chain), then the distance between the layers will be 30-32 Å , an observation consistent with the lamellar spacing of 29.8 and 32.0 Å observed for wire and thin-film, respectively. As mentioned above, thin-films show extra diffractions at q = 0.381, 0.761 Å^{-1}, and 0.2811 Å^{-1}. The first two peaks are attributable to the 1st and 2nd order peaks of 16.5 Å for a regular structure at the angle of 69° from the surface normal, while the third diffraction corresponds to an interlayer spacing of 22.4 Å for layer structure. These results suggest that a conjugation unit of a **DPP(3HT)$_2$** molecule is oriented at an angle of 69° to the central rigid backbone (see a schematic model on the right in Fig. 3b, inset, enlarged one in Fig. S5. ESI‡) such that the vertical and lateral interlayer spacing values are 22.4 Å and 16.5 Å , respectively. Based on the abovementioned results of structural analysis, it can be inferred that a conjugation unit in **DPP(3HT)$_2$** films exhibit both parallel and pseudo-perpendicular (~69°) geometry to the surface, while wires show only one parallel geometry. Considering the structural characteristics of **DPP(3HT)$_2$** wires and thin-films, it can be inferred that wires with single crystal-like features will

inevitably lead to much efficient charge transport compared to thin-film with amorphous-like feature and two mixed crystal structures. In practice, this favorable molecular packing of **DPP(3HT)$_2$** is reflected in terms of the high hole carrier mobilities for highly ordered wire-based OFETs as opposed to the thin-film based OFETs (Table S1, ESI‡). Furthermore, in order to confirm our interpretation of the parallel geometry of **DPP(3HT)$_2$** wires, their 2D-GIXD patterns were calculated by means of the software ANAELU[11] as shown in Fig. 3d, based on the characteristics of a triclinic unit cell with a = 30.06 Å , b = 10.89 Å , c = 5.06 Å, α = 79.3°, β = 88.3°, and γ = 88.7°. It is clearly seen that the measured diffraction pattern for wires is consistent with the calculated diffraction pattern, with the exception of spot-like features (Fig S6, ESI‡).

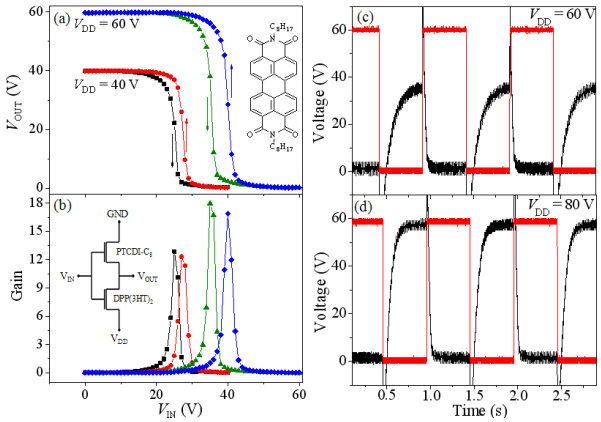

Fig. 4 Static (a-b) and dynamic (c-d) response of the complementary inverter based on crystalline wires based OFETs with CL-PVP gate dielectric. **DPP(3HT)$_2$** and PTCDI-C_8 are the *p*- and *n*-channels, respectively.

A simple logic circuit, a complementary inverter (inset of Fig. 4b), was constructed by combining *p*-(**DPP(3HT)$_2$** wire) and *n*-channel (PTCDI-C_8 wire, inset of Fig. 4a) OFETs with CL-PVP gate dielectric (Fig S7, ESI‡). Figs. 4a and b show the typical voltage transfer curve (V_{IN} vs V_{OUT}) and the corresponding gain from 0 to 60 V at two V_{DD}s (40 V and 60 V). The inverter shows good inversion with small hysteresis in air with a maximum gain (dV_{OUT}/dV_{IN}), which is the switch speed of the device, of 18 at V_{IN} = 35 V. The high gain and the lower hysteresis of the device in air indicates **DPP(3HT)$_2$** wires could be used in more complex logic circuits. We also measured the dynamic response characteristics of the inverter at an input frequency of 1 Hz, at V_{DD} of 60 V (Fig. 4c) and 80 V (Fig. 4d). It was found that the inverter exhibits good inversion to V_{IN} for both values of V_{DD} (60 V and 80 V).

We successfully fabricated **DPP(3HT)$_2$** wire-based OFETs and complementary inverters, and analyzed the performance of these device. Crystalline wire-based OFETs showed much better device performance than did thin-film based devices owing to the high homogeneity of crystal structure in **DPP(3HT)$_2$** wires. That is, while the wire exhibits only one parallel geometry, the thin-film exhibits both parallel and pseudo-perpendicular (~69°) geometries leading to the high difference in the charge transport properties of the respective devices. Finally, organic complementary inverters based on **DPP(3HT)$_2$** (*p*-channel) and PTCDI-C_8 (*n*-channel) wires were fabricated on polymer gate dielectric and inversion characteristics were investigated, that is the first report on 1D-microwire of molecular DPP.

This work was supported by the National Research Foundation (NRF) funded by the Korea Government (MEST) (R11-2008-052-03003, 2012R1A2A2A01045694). A.K.P. acknowledges financial support from the KU Brain Pool Program of Konkuk University.

Notes and references

[a]*Department of Chemistry, Konkuk University, 120 Neungdong-ro, Gwangjin-gu, Seoul 143-701, Republic of Korea. Email: pyosm@konkuk.ac.kr;* [b]*Pohang Accelerator Laboratory, Pohang, 790-784, Republic of Korea*.

†These authors have equally contributed to this work.

‡Electronic Supplementary Information (ESI) available: Materials, device fabrication and characterization details. See DOI: 10.1039/c000000x/

1 S. Hotta, T. Yamao, S. Z. Bisri, T. Takenobu and Y. Iwasa, *J. Mater. Chem. C*, 2014, **2**, 965; E. M. Garcia-Frutos, *J. Mater. Chem. C*, 2013, **1**, 3633; A. K. Palai, H. Cho, S. Cho, T. Shin, S. Jang, S.-U. Park and S. Pyo, *Org. Electron.*, 2013, **14**, 1396; X. Liu, Y. Wang, J. Gao, L Jiang, X. Qi, W. Hao, S. Zou, H. Zhang, H. Li and W. Hu, *Chem. Commun.*, 2014, **50**, 442; J.-P. Hong, M.-C. Um, S.-R. Nam, J.-I. Hong and S. Lee, *Chem. Commun*. 2009, 310.

2 O. Knopfmacher, M. L. Hammock, A. L. Appleton, G. Schwartz, J. Mei, T. Lei, J. Pei and Z. Bao, *Nat. Commun.*, 2014, 5:2954 DOI: 10.1038/ncomms3954; M. S. Chen, O. P. Lee, J. R. Niskala, A. T. Yiu, C. J. Tassone, K. Schmidt, P. M. Beaujuge, S. S. Onishi, M. F. Toney, A. Zettl and J. M. J. Frechet, *J. Am. Chem. Soc.*, 2013, **135**, 19229; J. H. Kim, D. H. Lee, D. S. Yang, D. U. Heo, K. H. Kim, J. Shin, H.-J. Kim, K.-Y. Baek, K. Lee, H. Baik, M. J. Cho and D. H. Choi, *Adv. Mater.*, 2013, **25**, 4102; K. Shi, T. Lei, X.-Y. Wang, J.-Y. Wang and J. Pei, *Chem. Sci.*, 2014, **5**, 1041; C. Fan, A. P. Zoombelt , H. Jiang, W. Fu , J. Wu, W. Yuan, Y. Wang, H. Li, H. Chen and Z. Bao, *Adv. Mater.*, 2013, **25**, 5762.

3 S. Loser, H. Miyauchi, J. W. Hennek, J. Smith, C. Huang, A. Facchetti and T. J. Marks, *Chem. Commun.*, 2012, **48**, 8511; P. Sonar, T. R. B. Foonga and A. Dodabalapur, *Phys. Chem. Chem. Phys.*, 2014, **16**, 4275; M. Kaur, D. S. Yang, J. Shin, T. W. Lee, K. Choi, M. J. Cho and D. H. Choi, *Chem. Commun.*, 2013, **49**, 5495; P. Sonar, T.-J. Ha and A. Dodabalapur, *Chem. Commun.*, 2013, **49**, 1588.

4 H. Liu, H. Jia, L. Wang, Y. Wu, C. Zhan, H. Fu and J. Yao, *Phys. Chem. Chem. Phys.*, 2012, **14**, 14262.

5 M. Tantiwiwat, A. Tamayo, N. Luu, X.-D. Dang and T.-Q. Nguyen, *J. Phys. Chem. C*, 2008, **112**, 17402.

6 W. S. Yoon, S. K. Park, I. Cho, J.-A. Oh, J. H. Kim and S. Y. Park, *Adv. Funct. Mater.*, 2013, **23**, 3519.

7 B. Mukherjee, K. Sim, T. J. Shin, J. Lee, M. Mukherjee, M. Ree and S. Pyo, *J. Mater. Chem.*, 2012, **22**, 3192.

8 A. K. Palai, J. Lee, M. Jea, H. Na, T. J. Shin, S. Jang, S.-U. Park and S. Pyo, *J. Mater. Sci.*, 2014, **49**, 4215.

9 A. K. Palai, J. Lee, S. Das, J. Lee, H. Cho, S. -U. Park and S. Pyo, Org. Electron., 2012, **13**, 2553.

10 S. Loser, C. J. Bruns, H. Miyauchi, R. P. Ortiz, A. Facchetti, S. I. Stupp and T. J. Marks, *J. Am. Chem. Soc.*, 2011, **133**, 8142.

11 L. Fuentes-Montero, M. E. Montero-Cabrera and L. Fuentes-Cobas, *J. Appl. Cryst.*, 2011, **44**, 241.